Ultrasonic Attenuation in Polycrystalline Materials in 2D

(article starts on next page)

Ultrasonic Attenuation in Polycrystalline Materials in 2D

Anders Boström[1] · Aurlia Ruda[2]

Abstract

Grains in a polycrystalline material, typically a metal, act as scatterers of ultrasonic waves and thus give rise to attenuation of the waves. Grains have anisotropic stiffness properties, typically orthotropic or cubic. A new approach is proposed to calculate attenuation in a 2D setting starting from the scattering by an anisotropic circle in an isotropic surrounding. This problem has recently been solved, giving explicit, simple expressions for the elements of the transition (T) matrix (which gives the relation between the the incoming and scattered fields) when the circle is small compared to the ultrasonic wavelengths. The T matrix can be used to calculate the total scattering cross section, which in turn can be used to estimate the attenuation in the material. Explicit expressions for the attenuation coefficient for longitudinal and transverse waves are obtained for a cubic material, and contrary to results in the literature these expressions are valid also for strong anisotropy. For the longitudinal attenuation coefficient a comparison with recent FEM results for Inconel 600 gives excellent agreement.

Keywords Ultrasonic attenuation · 2D · Cubic material

1 Introduction

Grains in a polycrystalline material, typically a metal, act as scatterers of ultrasonic waves and thus give rise to attenuation of the waves. A model of the attenuation is useful to characterize polycrystalline materials by inversion from attenuation measurements. In ultrasonic nondestructive testing the scattering induced grain noise is also of importance. To estimate the attenuation and effective wave speed in polycrystals various approximate methods have been used. As examples Stanke and Kino [1] calculate the wave speed and attenuation using a perturbation method with weak anisotropy and give an excellent review of work prior to 1984, Hirsekorn [2] performs a similar analysis for textured materials (giving an anisotropic effective material), Thompson et al. [3]

✉ Anders Boström
anders.bostrom@chalmers.se

Aurlia Ruda
aurelia.ruda@ens-paris-saclay.fr

1 Department of Mechanics and Maritime Sciences, Chalmers University of Technology, Gothenburg, Sweden

2 ENS Cachan, Universit Paris-Saclay, 61 avenue du Prsident Wilson, 94235 Cachan cedex, France

give an overview of scattering of elastic waves in simple and complex polycrystals, and Li and Rokhlin [4] study the scattering in general random anisotropic solids. These studies all use volume integral equation methods combined with some perturbation method, most often the Born approximation (which means a restriction to weak anisotropy). Recently finite element methods (FEM) have been used to compute the attenuation and effective wave speed in polycrystalline materials, see Van Pamel et al. [5–7] and Ryzy et al. [8]. For excellent and more extensive introductions (and many further references) these papers [1,5–8] can be consulted.

Here a different approach is proposed, where first the scattering by a single anisotropic grain in an effective isotropic surrounding is studied. The effective stiffnesses of the surrounding material are taken as the Voigt averages of the stiffnesses of the grain, see Van Pamel et al. [7] for a discussion of the appropriateness of this. Only the 2D problem for in-plane (P and SV) waves is treated and the grains are assumed to be cubic, this being the simplest and most common case. The grains are assumed small compared to the wavelength, usually called the Rayleigh regime, so it should be enough to assume them to be circular (the scattering at low frequencies is predominantly a volume effect, see Yang et al. [9] and Ryzy et al. [8]), and this case has recently been solved by Boström [10], giving simple explicit expressions. The simplest possible approach to estimate the attenuation is

investigated and this yields a simple expression for the attenuation coefficient. It is, in particular, noted that the present approach does not assume weak anisotropy, a restriction that is made by other analytical approaches.

2 Scattering by an Anisotropic Circle

Consider the scattering of elastic P-SV waves by an anisotropic circle of radius a residing in an isotropic medium. This problem has recently been solved by Boström [10] and here only the pertinent results are repeated. The material inside the circle is taken as cubic with stiffness constants c_1, c_3, and c_4, so that the constitutive equations are

$$\sigma_{xx} = c_1 \epsilon_{xx} + c_3 \epsilon_{yy},$$
$$\sigma_{yy} = c_3 \epsilon_{xx} + c_1 \epsilon_{yy},$$
$$\sigma_{xy} = 2c_4 \epsilon_{xy},$$

where the x and y axes are along the principal directions. The density inside the circle is ρ_0. The effective material surrounding the circle has the same density ρ_0 and Lamé parameters λ_0 and μ_0. These are taken as the Voigt averages, thus

$$\lambda_0 = \frac{1}{4}(c_1 + 3c_3 - 2c_4),$$
$$\mu_0 = \frac{1}{4}(c_1 - c_3 + 2c_4).$$

Only time harmonic situations are considered and the time factor $\exp(-\mathrm{i}\omega t)$, where ω is the angular frequency and t is time, is suppressed throughout. The longitudinal (pressure, P) wave number is $k_p = \omega\sqrt{\rho_0/(\lambda_0 + 2\mu_0)}$ and the transverse (shear, S) is $k_s = \omega\sqrt{\rho_0/\mu_0}$.

To expand the incident and scattered wave polar coordinates r,φ are employed and the following wavefunctions are introduced

$$
\begin{aligned}
\boldsymbol{\chi}^0_{1\sigma m}(\boldsymbol{r}) &= \sqrt{\epsilon_m}\,(1/k_s)\nabla \times \left[\boldsymbol{e}_z \mathrm{J}_m(k_s r)\begin{pmatrix} \sin m\varphi \\ -\cos m\varphi \end{pmatrix}\right] \\
&= \sqrt{\epsilon_m}\left[\boldsymbol{e}_r \frac{m}{k_s r}\mathrm{J}_m(k_s r)\begin{pmatrix} \cos m\varphi \\ \sin m\varphi \end{pmatrix} \right. \\
&\quad \left. -\boldsymbol{e}_\varphi \mathrm{J}'_m(k_s r)\begin{pmatrix} \sin m\varphi \\ -\cos m\varphi \end{pmatrix}\right],
\end{aligned}
\tag{1}
$$

$$
\begin{aligned}
\boldsymbol{\chi}^0_{2\sigma m}(\boldsymbol{r}) &= \sqrt{\epsilon_m}\,(1/k_s)\nabla \left[\mathrm{J}_m(k_p r)\begin{pmatrix} \cos m\varphi \\ \sin m\varphi \end{pmatrix}\right] \\
&= \sqrt{\epsilon_m}\,(k_p/k_s)\left[\boldsymbol{e}_r \mathrm{J}'_m(k_p r)\begin{pmatrix} \cos m\varphi \\ \sin m\varphi \end{pmatrix} \right. \\
&\quad \left. -\boldsymbol{e}_\varphi \frac{m}{k_p r}\mathrm{J}_m(k_p r)\begin{pmatrix} \sin m\varphi \\ -\cos m\varphi \end{pmatrix}\right].
\end{aligned}
\tag{2}
$$

Here the first index 1 or 2 on the wavefunctions denotes transverse or longitudinal waves, respectively. The second index $\sigma = e$ (even) or o (odd) corresponds to the upper or lower row, respectively, of the trigonometric functions and gives waves which are symmetric or antisymmetric, respectively, with respect to $\varphi = 0$. The Neumann factor is $\epsilon_0 = 1$ and $\epsilon_m = 2$ for $m = 1, 2, \ldots$. For $m = 0$ there are just two wavefunctions, one odd for $\tau = 1$ and one even for $\tau = 2$. The upper index 0 on the wave functions denotes that they are regular, containing a Bessel function J_m, the corresponding outgoing wavefunctions contain a Hankel function $\mathrm{H}_m^{(1)}$ and are denoted by an upper index +. The unit vectors are denoted $\boldsymbol{e}_r$, $\boldsymbol{e}_\varphi$, and $\boldsymbol{e}_z$.

A general way to represent the scattering by the circle is to calculate its T (transition) matrix, which relates the expansion coefficients of the scattered wave to those of the incident wave. Out to its sources (everywhere for a plane wave) the incident wave can be expanded in terms of regular wavefunctions

$$\boldsymbol{u}^{\text{in}} = \sum_{\tau,\sigma,m} a_{\tau\sigma m}\boldsymbol{\chi}^0_{\tau\sigma m}, \tag{3}$$

where the summation is over $\tau = 1, 2$, $\sigma = e, o$, and $m = 0, 1, \ldots$, and $a_{\tau\sigma m}$ are the expansion coefficients that specifies the incident wave. The scattered wave satisfies radiation conditions and can be expanded in terms of outgoing wavefunctions

$$\boldsymbol{u}^{\text{sc}} = \sum_{\tau,\sigma,m} f_{\tau\sigma m}\boldsymbol{\chi}^+_{\tau\sigma m}, \tag{4}$$

where $f_{\tau\sigma m}$ are the expansion coefficients of the scattered wave. The relation between the scattered and incident waves defines the transition matrix

$$f_{\tau\sigma m} = \sum_{\tau',\sigma',m'} T_{\tau\sigma m,\tau'\sigma'm'} a_{\tau'\sigma'm'}. \tag{5}$$

The transition matrix becomes symmetric with the present definition of the wave functions.

The constitutive equations inside the circle are expressed in Cartesian coordinates. To be able to apply the boundary conditions at the circular boundary it is much more convenient to have solutions in polar coordinates and the constitutive equations are therefore transformed to polar coordinates

$$
\begin{aligned}
\sigma_{rr} &= (\lambda_0 + 2\mu_0)\epsilon_{rr} + \lambda_0\epsilon_{\varphi\varphi} + \beta\left(\cos 4\varphi\left(\epsilon_{rr} - \epsilon_{\varphi\varphi}\right)\right. \\
&\quad \left. -2\sin 4\varphi\,\epsilon_{r\varphi}\right),
\end{aligned}
\tag{6}
$$
$$
\begin{aligned}
\sigma_{\varphi\varphi} &= \lambda_0\epsilon_{rr} + (\lambda_0 + 2\mu_0)\epsilon_{\varphi\varphi} + \beta\left(\cos 4\varphi\left(\epsilon_{\varphi\varphi} - \epsilon_{rr}\right)\right. \\
&\quad \left. +2\sin 4\varphi\,\epsilon_{r\varphi}\right),
\end{aligned}
\tag{7}
$$
$$\sigma_{r\varphi} = 2\mu_0\epsilon_{r\varphi} + \beta\left(\sin 4\varphi\left(\epsilon_{\varphi\varphi} - \epsilon_{rr}\right)\right.$$

$$-2\cos 4\varphi\, \epsilon_{r\varphi}\big). \tag{8}$$

It is noted that the Voigt averages here naturally appear in the terms with no angular dependence. The following anisotropy factor is introduced (essentially the same as introduced by many others)

$$\beta = \frac{1}{4}\left(c_1 - c_3 - 2c_4\right). \tag{9}$$

In the present case with a 2D cubic material there is only coupling between different azimuthal orders (m values) in steps of 4, in the case of 2D orthotropy there is a further coupling in steps of 2, see Boström [10].

The displacement field inside the circle is divided into four independent parts due to the symmetries. Thus the four parts are symmetric or antisymmetric with respect to the x and y axes. Here a symmetric displacement with respect to the x axis has an even x component and an odd y component and vice versa for symmetry with respect to the y axis. This also means that a symmetric displacement with respect to the x axis has an even r component and an odd φ component and vice versa for symmetry with respect to the y axis. The doubly symmetric wavefunctions have $\sigma = e$ and $m = 0, 2, 4, \ldots$, the symmetric-antisymmetric (with respect to the x and y axes, respectively) ones have $\sigma = e$ and $m = 1, 3, \ldots$, the antisymmetric-symmetric ones have $\sigma = o$ and $m = 1, 3, \ldots$, and the doubly antisymmetric ones have $\sigma = o$ and $m = 0, 2, 4, \ldots$. Thus, there is no coupling between these four groups, meaning that the corresponding T matrix elements vanish.

The displacement components inside the circle can be expanded in trigonometric series in the azimuthal coordinate appropriate to the symmetry of the component. A power series in the radial coordinate is then assumed and recursion relations can be set up for the expansion coefficients in these series, essentially solving the problem inside the circle.

To determine the T matrix, continuity of displacement and traction at $r = a$ is set up and the resulting systems are solved for the expansion coefficients of the scattered field, see Boström [10] for details. In the present case, with cubic grains and a surrounding effective medium with the same density as the grains and stiffness constants determined as Voigt averages, the expressions for the T matrix elements simplify considerably. To leading order at low frequencies the equal densities mean that there is no scattering at all for the symmetric–antisymmetric and antisymmetric–symmetric parts. The monopole $m = 0$ part vanishes for a cubic material as does the coupling parts between the monopole $m = 0$ and quadrupole $m = 2$. Finally the quadrupole parts for $m = m' = 2$ are the same for the symmetric–symmetric and antisymmetric–antisymmetric parts. These leading order T matrix elements

become

$$T_{1\sigma 2, 1\sigma 2} = \frac{k_s^4 a^2}{k_p^2}\frac{\mathrm{i}\pi\beta}{M}, \tag{10}$$

$$T_{1\sigma 2, 2\sigma 2} = T_{2\sigma 2, 1\sigma 2} = k_s^2 a^2 \frac{\mathrm{i}\pi\beta}{M}, \tag{11}$$

$$T_{2\sigma 2, 2\sigma 2} = k_p^2 a^2 \frac{\mathrm{i}\pi\beta}{M}, \tag{12}$$

where

$$M = 8(\lambda_0 + 2\mu_0) + 4\beta(3 + \lambda_0/\mu_0), \tag{13}$$

and $\sigma = e, o$. As noted by others, the S wave scattering is much stronger than the P wave scattering at low frequencies.

3 The Attenuation Coefficient

To estimate the attenuation only the simplest approach is used. All multiple scattering is neglected and as mentioned the scattering by each grain is supposed to take place in an isotropic medium with the Voigt effective stiffness constants of the material (but ignoring the attenuation in the material). The scattering by each grain is given by its total scattering cross section, a measure (a length in 2D) which gives the part of an incident plane wave that is scattered by the grain and thus lost to the coherent wave. This gives an estimation in 2D of the attenuation coefficient α as (see Zhang and Gross [12])

$$\alpha = \frac{1}{2}n\gamma = \frac{c\gamma}{2\pi a^2}. \tag{14}$$

Here n is the number density of grains, γ is the total scattering cross section, and c is the relative density of grains. This formula for the attenuation is usually supposed to be valid only for dilute concentrations, typically $c < 0.05$ or less. As the grains fill the whole volume $c = 1$ is used. The rationale for this is that each grain scatters extremely little in the low frequency limit. This approach has been used also by others, see references in Stanke and Kino [1]. A schematic picture of the model is given in Fig. 1.

It is straightforward to calculate the total scattering cross section, see Varadan et al. [11]. The result is that for an incident P wave it is

$$\gamma^P = \frac{4k_p}{k_s^2}\sum_{\sigma m}\left(|f_{1\sigma m}|^2 + |f_{2\sigma m}|^2\right), \tag{15}$$

and for an incident S wave

$$\gamma^S = \frac{4}{k_s}\sum_{\sigma m}\left(|f_{1\sigma m}|^2 + |f_{2\sigma m}|^2\right). \tag{16}$$
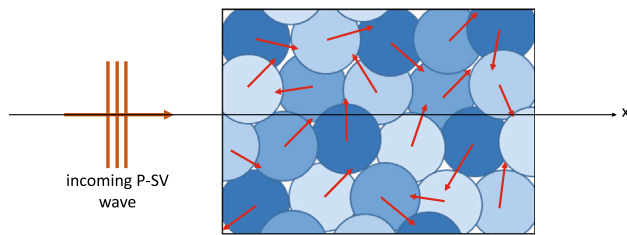
Fig. 1 A schematic of the model with a collection of partially overlapping circles with random orientation (indicated by arrows) of the grains

These are expressed in the expansion coefficients of the scattered wave $f_{\tau\sigma m}$. Expressing these coefficients in terms of the T matrix and the expansion coefficients of the incident wave, performing an average over all directions of incidence (which is the same as a random orientation of the grains), and specializing to the anisotropic circle at low frequencies without contrast in density to the surrounding, this simplifies and gives the attenuation coefficients (with the notation from the preceding section)

$$\alpha^P = \frac{2k_p^3}{\pi k_s^4 a^2} \left(|T_{1o2,2o2}|^2 + |T_{1e2,2e2}|^2 \right.$$
$$\left. + |T_{2o2,2o2}|^2 + |T_{2e2,2e2}|^2 \right), \qquad (17)$$

$$\alpha^S = \frac{2}{\pi k_s a^2} \left(|T_{1o2,1o2}|^2 + |T_{1e2,1e2}|^2 \right.$$
$$\left. + |T_{2o2,1o2}|^2 + |T_{2e2,1e2}|^2 \right). \qquad (18)$$

Here all the T matrix elements are given explicitly in simple form in the preceding section. Inserting these and simplifying, the final result is

$$\alpha^P = \frac{\pi a^2 \beta^2 k_p^3}{(2(\lambda_0 + 2\mu_0) + \beta(3 + \lambda_0/\mu_0))^2} \left[1 + \left(\frac{k_p}{k_s} \right)^4 \right], \qquad (19)$$

$$\alpha^S = \frac{\pi a^2 \beta^2 k_s^3}{(2(\lambda_0 + 2\mu_0) + \beta(3 + \lambda/\mu_0))^2} \left[1 + \left(\frac{k_s}{k_p} \right)^4 \right]. \qquad (20)$$

These attenuation coefficients depend on frequency to the third power and the grain radius squared as expected, see Van Pamel et al. [6]. As the shear wave number is roughly twice the compressional one, the shear wave attenuation coefficient is larger that the compressional one with about the factor $(k_s/k_p)^7$. It is of interest to note that it is only the quadrupole terms (of azimuthal order $m = 2$) that contributes to the attenuation.

The Unified theory of Stanke and Kino [1] is often used as a reference. This is a 3D theory valid for all frequencies, however, it is a perturbation approach assuming weak anisotropy.

Table 1 Material constants for four materials (obtained from References [1] and [5]) and the error in making a linearization in the attenuation coefficients

Materials	Copper	Inconel 600	Iron	Aluminium
c_1 (GPa)	176.2	234.6	219.2	103.4
c_3 (GPa)	124.9	145.4	136.8	57.1
c_4 (GPa)	81.8	126.2	109.2	28.6
ρ (kg/m^3)	8970	8260	7860	2760
λ_0 (GPa)	96.8	104.6	102.0	54.4
μ_0 (Gpa)	53.7	85.4	75.2	25.9
β (Gpa)	−28.1	−40.8	−34.0	−2.7
ν (−)	−1.37	−1.29	−1.24	−0.38
Linear error (%)	33	31	26	6.6

In the Rayleigh regime their result for the P wave attenuation coefficient can be written [1]

$$\alpha^P = \frac{\frac{4}{3}\pi a^3}{375\pi} (k_p)^4 \frac{\nu^2 c_4^2}{(\lambda_0 + 2\mu_0)^2} \left[1 + \frac{3}{2} \left(\frac{k_s}{k_p} \right)^5 \right]. \qquad (21)$$

Here $\nu = 4\beta/c_4$ is a dimensionless anisotropy coefficient. This result should thus be valid for small ν (and low frequencies). Comparing this attenuation coefficient with Eq. (19) there are both similarities and differences. The difference in dependence on frequency and radius is to be expected due to the 2D and 3D assumption. That the last factor (inside the square brackets) is different is a little surprising, but in fact leads to that the two results are similar numerically. The extra term in β in the denominator in Eq. (19) is very interesting. A similar term is missing in Eq. (21) because of the perturbation approach. As seen below this term is of importance if the anisotropy is strong.

Table 1 shows the material constants for copper, Inconel 600, iron, and aluminium, all of which have cubic grains. First the three stiffness constants c_1, c_3, c_4 of the cubic grains are given, followed by the Voigt averages λ_0 and μ_0 and the anisotropy parameter β. The more common dimensionless anisotropy parameter ν follows, where the latter is a measure of the degree of anisotropy, with $\nu = 0$ giving an isotropic material.

Other analytical approaches in the literature demand small anisotropy, either through a perturbation method in ν or by using the Born approximation. In contrast the present method does not have such a limitation, instead the main limitation is that the Rayleigh regime is assumed. It can therefore be of interest to see the error induced by a linearization of the present result. This amounts to putting $\beta = 0$ in the denominator in Eqs. (19) and (20). The relative error $|\alpha_{\text{lin}}^P - \alpha^P|/\alpha^P$, where α_{lin}^P is the linearized form of α^P, is therefore also given in Table 1. For the materials listed it is seen that this error ranges from 6.6% for aluminium, which is

Fig. 2 2D normalised longitudinal attenuation coefficient versus normalised frequency in the Rayleigh regime for polycrystalline Inconel 600. The present result is compared to 2D FEM [5] and 3D Unified theory [1]
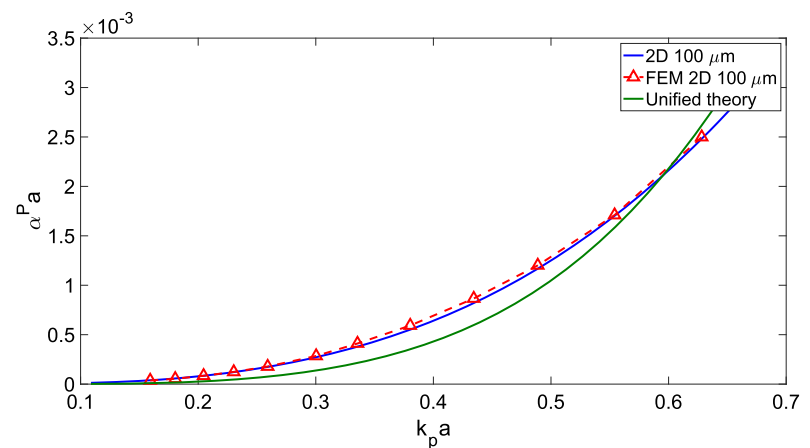
rather weakly anisotropic, to 33% for copper, which is rather strongly anisotropic. Except for aluminium this error is quite substantial.

Recently, FEM has been used to model attenuation due to grain scattering in both 2D and 3D [5–8]. The only result that can be compared with the present one are the 2D longitudinal result for Inconel 600 of Van Pamel et al. [5]. Figure 2 shows the normalized longitudinal attenuation coefficient for Inconel 600 (material properties given in Table 1) as a function of normalized frequency in the Rayleigh regime for the present result and 2D FEM [5]. Also the 3D result of the Unified theory is shown. The grain radius is $a = 100\,\mu\text{m}$. The agreement between the present result and 2D FEM is excellent, the difference is about 5% at most, thus validating the present approach and the assumptions that are made (circular grains and neglect of multiple scattering). The unified theory is of the same order of magnitude, but as the frequency dependence is different the results must of course differ. It should be noted that the results are sensitive to the grain radius a. The present result assumes that all grains have the same radius and the 2D FEM result [5] seems to be for a case where the grain size is very uniform (more than would normally be the case in a real material).

4 Concluding Remarks

In the present paper simple expressions are derived for the longitudinal and transverse attenuation coefficients in 2D for a cubic polycrystalline material. The material may be strongly anisotorpic, instead the main limitation is that the result is only valid in the Rayleigh regime. It is also assumed that all the grains are circular with the same radius and that multiple scattering can be neglected, but these two limitations should be of minor importance as the comparison with FEM shows.

The main advantage of the present approach compared to previous results in the literature is that the anisotropy can

be arbitrarily strong. A further advantage with the present approach is that it is straightforward to generalize it in various directions. Thus it is straightforward to consider a distribution of grain sizes, cf. Arguelles and Turner [13], or to consider grains of different types (as in a duplex material). It is also possible to include a distribution of inclusions of other types, like pores or cracks.

To be of real practical value the present approach should be generalized to 3D; such work is in progress.

References

1. Stanke, F.E., Kino, G.S.: A unified theory for elastic wave propagation in polycrystalline materials. J. Acoust. Soc. Am. **75**, 665–681 (1984)
2. Hirsekorn, S.: Directional dependence of ultrasonic propagation in textured polycrystals. J. Acoust. Soc. Am. **79**, 1269–1279 (1986)
3. Thompson, R.B., Margetan, F.J., Haidipur, P., Yu, L., Li, A., Panetta, P., Wasan, H.: Scattering of elastic waves in simple and complex polycrystals. Wave Motion **45**, 655–674 (2008)
4. Li, J., Rokhlin, S.I.: Elastic wave scattering in random anisotropic solids. Int. J. Solids Struct. **78–79**, 110–124 (2016)
5. Van Pamel, A., Brett, C.R., Huthwaite, P., Lowe, M.J.S.: Finite element modelling of elastic wave scattering within a polycrystalline material in two and three dimensions. J. Acoust. Soc. Am. **138**, 2326–2336 (2015)
6. Van Pamel, A., Sha, G., Rokhlin, S.I., Lowe, M.J.S.: Finite-element modelling of elastic wave propagation and scattering within heterogeneous media. Proc. R. Soc. A **473**, 20160738 (2016)
7. Van Pamel, A., Sha, G., Lowe, M.J.S., Rokhlin, S.I.: Numerical and analytical modelling of elastodynamic scattering within polycrystalline materials. J. Acoust. Soc. Am. **143**, 2394–2408 (2018)
8. Ryzy, M., Grabec, T., Sedlak, P., Veres, I.A.: Influence of grain morphology on ultrasonic wave attenuation in polycrystalline media

with statistically equiaxed grains. J. Acoust. Soc. Am. **143**, 219–229 (2018)

9. Yang, L., Lobkis, O.I., Rokhlin, S.I.: An integrated model for ultrasonic wave propagation and scattering in a polycrystalline medium with elongated hexagonal grains. Wave Motion **49**, 544–560 (2012)

10. Boström, A.: Scattering of in-plane elastic waves by an anisotropic circle. Q. J. Mech. Appl. Math. **71**, 139–155 (2018)

11. Varadan, V.V., Lakhtakia, A., Varadan, V.K.: *Field Representations and Introduction to Scattering, Vol. 1 in Acoustic, Electromagnetic and Elastic Wave Scattering*. North-Holland (1991)

12. Zhang, C., Gross, D.: On wave propagation in elastic solids with cracks. Computational Mechanics Publications, Cambridge (1998)

13. Arguelles, A.P., Turner, J.A.: Ultrasonic attenuation of polycrystalline materials with a distribution of grain sizes. J. Acoust. Soc. Am. **141**, 4347–4353 (2017)